Cerebral Cortex Advance Access published January 9, 2014

Cerebral Cortex
doi:10.1093/cercor/bht352

The Role of Fronto-Parietal and Fronto-Striatal Networks in the Development of Working Memory: A Longitudinal Study

Fahimeh Darki and Torkel Klingberg

Department of Neuroscience, Karolinska Institutet, Stockholm, Sweden

Address correspondence to Torkel Klingberg, Department of Neuroscience, Karolinska Institutet, Developmental Cognitive Neuroscience Lab, Retzius Väg 8, Room A3-312, 17 177 Stockholm, Sweden. Email: torkel.klingberg@ki.se

The increase in working memory (WM) capacity is an important part of cognitive development during childhood and adolescence. Cross-sectional analyses have associated this development with higher activity, thinner cortex, and white matter maturation in fronto-parietal networks. However, there is still a lack of longitudinal data showing the dynamics of this development and the role of subcortical structures. We included 89 individuals, aged 6–25 years, who were scanned 1–3 times at 2-year intervals. Functional magnetic resonance imaging (fMRI) was used to identify activated areas in superior frontal, intraparietal cortices, and caudate nucleus during performance on a visuo-spatial WM task. Probabilistic tractography determined the anatomical pathways between these regions. In the cross-sectional analysis, WM capacity correlated with activity in frontal and parietal regions, cortical thickness in parietal cortex, and white matter structure [both fractional anisotropy (FA) and white matter volume] of fronto-parietal and fronto-striatal tracts. However, in the longitudinal analysis, FA in white matter tracts and activity in caudate predicted future WM capacity. The results show a dynamic of neural networks underlying WM development in which cortical activity and structure relate to current capacity, while white matter tracts and caudate activity predict future WM capacity.

Keywords: caudate nucleus, cortical thickness, development, DTI, fMRI, working memory

Introduction

Working memory (WM) capacity increases during childhood and adolescence, which is important for academic performance and cognition (Gathercole et al. 2003; Dumontheil and Klingberg 2012). Impaired WM capacity is associated with several developmental neuropsychiatric and learning disorders, including attention-deficit/hyperactivity disorder (ADHD; Nigg 2001; Westerberg et al. 2004; Martinussen et al. 2005) and dyscalculia (McLean and Hitch 1999; Camos 2008; Szucs et al. 2013). It is therefore important to characterize the neural basis of this development.

WM capacity in children and adolescents is positively correlated with brain activity, most consistently localized to the intraparietal cortex, superior frontal sulcus, and dorsolateral prefrontal cortex (Klingberg et al. 2002; Kwon et al. 2002; Crone et al. 2006; Scherf et al. 2006; Olesen et al. 2007). Measures of cortical thinning in the frontal and parietal cortex are also correlated with WM capacity (Tamnes et al. 2010; Østby et al. 2011; Tamnes et al. 2013) and also with reasoning ability, which is an ability highly correlated with WM (Sowell et al. 2004; Shaw et al. 2006; Tamnes et al. 2011; Wendelken et al. 2011). Furthermore, white matter maturation of the pathways between the parietal and frontal cortex, including the superior longitudinal fasciculus, correlate with WM capacity during childhood and adolescence (Olesen, Nagy, et al. 2003; Nagy et al. 2004; Østby et al. 2011; Vestergaard et al. 2011).

These studies thus suggest that improvements in WM capacity are associated with a gradual maturation of white and gray matter in a fronto-parietal network. It is not clear, however, how these changes are related to each other, and if certain changes cause the later changes in WM performance. The role of the striatum for development is also unclear. The caudate nucleus is activated during performance of WM tasks in nonhuman primates (Levy et al. 1997), children (Klingberg et al. 2002; Ziermans et al. 2012), and adults (Postle et al. 2000), but its role in development is unclear.

One reason why the dynamics of WM development has not been clarified is that most of these studies have been cross-sectional, correlating the current cognitive ability with current structure or activity. An exception here is the study by Ullman et al. (2014), who used a longitudinal design and a multivariate analysis to show that there were differences between multivariate models correlating with current cognitive capacity and the models predicting the change of capacity over the next 2 years. Since this study was multivariate, it was not designed to specify the role of anatomically defined regions or networks.

In the current study, we first identified the regions of interest (ROIs) based on the main effect of WM during development (Dumontheil et al. 2011; Ziermans et al. 2012) for a group of 89 individuals, aged 6–25 years, who were scanned 1–3 times at 2-year intervals. Using diffusion tensor imaging (DTI), we then traced the white matter tracts connecting these regions. Measures of blood-oxygen-level dependent (BOLD) contrast and cortical thickness were extracted from functionally defined ROIs. White matter volume and fractional anisotropy (FA) were also measured along the fronto-parietal and front-striatal white matter pathways. The brain measures together with visuo-spatial WM capacity were assessed for 3 time points with 2-year intervals and used to characterize the relationship between brain and WM during development.

Methods

Participants

Eighty-nine typically developing children and young adults (6–25 years old) were selected randomly from participants in a larger, behavioral longitudinal study (Söderqvist et al. 2010). The subjects in the larger longitudinal study were randomly selected from the population registry in Nynäshamn. The data collection was conducted 3 times, each 2 years apart. The study was approved by the local ethics committee of the Karolinska University Hospital, Stockholm, Sweden. Informed consent was provided by the participants or the parents of children aged below 18 years old. Figure 1 shows the distribution of the included participants in all the behavioral and imaging assessments.

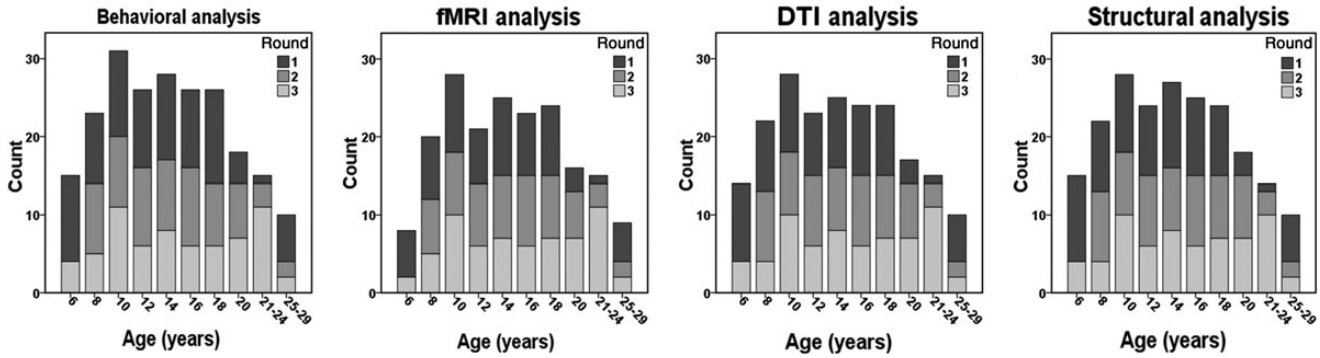

Figure 1. Distribution of the data for the different analyses across rounds 1, 2, and 3 of data collection, based on different age groups.

Assessment of Visuo-Spatial Working Memory

Visuo-spatial WM was assessed individually using a computerized Dot Matrix task from the Automated Working Memory Assessment (AWMA) battery (Alloway 2007). A number of dots in a four-by-four grid were displayed sequentially for 1000 ms, with a 500-ms interval. The task was to remember the location and the order of the dots. After few practice trials, the test started from the first level including one dot with 6 trials. By giving 4 correct responses, it continued to the next level where one more dot was added to the test. Three incorrect answers were the criteria for terminating the test on one level. The total number of correct trials was computed as a visuo-spatial WM score.

Brain Imaging and Analysis

Multimodal brain imaging and analyses were applied longitudinally to find the relationship between brain structure and function in WM-related networks. First, the functional magnetic resonance imaging (fMRI) ROIs were identified based on the main effect of WM during development. Then, the white matter pathways connecting these ROIs were traced using DTI data. Mean white matter volume and FA were computed along the white matter pathways. The BOLD contrast and cortical thickness were also extracted from functionally defined ROIs. Figure 2 illustrates the pipeline used for the multimodal image analyses, transformations between different modalities and the extraction of measures of interest.

Functional Brain Imaging and Processing

T_2*-weighted functional images were acquired on a 1.5-T Siemens scanner (Siemens, Erlangen, Germany) with a gradient-echo-planar imaging (EPI) sequence: time repetition (TR) = 3000 ms, time echo (TE) = 50 ms, field of view (FOV) of 220 × 220 mm^2, 64 × 64 matrix size, and 4.5 mm slice thickness. The same imaging sequence was applied for the second and third rounds of the study data collection, respectively, 2 and 4 years later. Participants performed 10 min of visuo-spatial WM task (Dumontheil et al. 2011) in the scanner. Dots were presented sequentially in a four-by-four grid, and the task was to remember the order and the position of a dot.

Preprocessing, first- and second-level analyses of the fMRI data were performed with SPM5 (www.fil.ion.ucl.ac.uk/spm/software/spm5) (Dumontheil et al. 2011; Ziermans et al. 2012). Functional images were first preprocessed by slice timing and motion correction. Then, the images were aligned and normalized to the Montreal Neurological Institute template and finally were high-pass (140 s) filtered and smoothed with a 12-mm Gaussian kernel.

Second-level analysis was performed using SPM5 for the group analysis of the WM contrast images using the flexible factorial design by considering subject and round of the scans as factors. After correcting for the effect of age and sex, the main WM contrast was performed at a false discovery rate (FDR) threshold of $P < 0.05$, to identify regions that were recruited during task performance. The activation map of main WM contrast, thresholded at FDR < 0.000001, was then split into smaller ROIs, so that each region was centered around a single local maximum. ROIs were defined so that individual regions did not overlap, and together covered the majority of the WM activation.

To implement the ROI-based functional and structural analyses on the fronto-parietal and fronto-striatal networks, 3 different functional ROIs, including the superior frontal, intraparietal (superior and inferior), and also the caudate nucleus were selected. Mean of the parameters estimated in the first-level analysis was computed for these significant clusters using MarsBar (Brett et al. 2002). The computed mean contrast values were then analyzed using a mixed linear model in an IBM SPSS statistics 21.0 software for the correlation and prediction assessments.

DTI and Probabilistic Fiber Tracking

DTI, with the scanning parameters of: FOV = 230 × 230 mm^2, matrix size = 128 × 128, 40 slices, 2.5 mm of slice thickness, and *b*-value of 1000 s/mm^2 in 64 gradient directions, was carried out at the third round of data collection of the longitudinal study. This was an additional sequence which was added to increase the resolution of the DT images and consequently to improve the tractography results. For the longitudinal assessment of white matter pathways, we used another sequence for which the data were available for all 3 rounds of data collection. This dataset was collected with a FOV of 230 × 230 mm^2, matrix size of 128 × 128, 19 slices with 6.5 mm thickness, and *b*-value of 1000 s/mm^2 in 20 gradient directions.

Eddy current and head motions were corrected with affine registration for all diffusion-weighted images to a reference volume using an FSL software (http://fsl.fmrib.ox.ac.uk/fsl/fslwiki/). The diffusion tensor parameters were then estimated for each voxel, and subsequently the DTI and FA data were constructed. Nonlinear registration was carried out using Tract-Based Spatial Statistics, TBSS v1.2, (http://fsl.fmrib.ox.ac.uk/fsl/fslwiki/TBSS) to align all FA images to the mean FA skeleton. To find the white matter pathways within the fronto-parietal and fronto-striatal networks, the functional ROIs (superior frontal, intraparietal, and caudate) were registered first to the mean FA image. In the next step, the back projection of the TBSS method was used to transform back the functional ROIs (Fig. 2*A*) to the DTI space of all individuals.

Probabilistic tractography was performed on all individuals' high-resolution DTI data (collected at the third round), initiating from all voxels within the seed masks using the probtrackx tool of FDT v2.0, FSL (http://fsl.fmrib.ox.ac.uk/fsl/fsl-4.1.9/fdt/fdt_probtrackx.html). For the fronto-striatal pathways, it began separately from the left and right caudate functionally defined regions by considering superior frontal as inclusion masks; whereas for fronto-parietal connections, the tractography initiated from the superior frontal and the inclusion masks were the intraparietal regions. The default parameters (5000 streamline samples, step length of 0.5 mm, and curvature threshold of 0.2) were used for the probabilistic fiber tracking. At the individual level, the tracts were thresholded by 5% of the samples to remove the voxels with low probability of connection (Leh et al. 2006). In the next step, all the traced white matter pathways were aligned using the TBSS

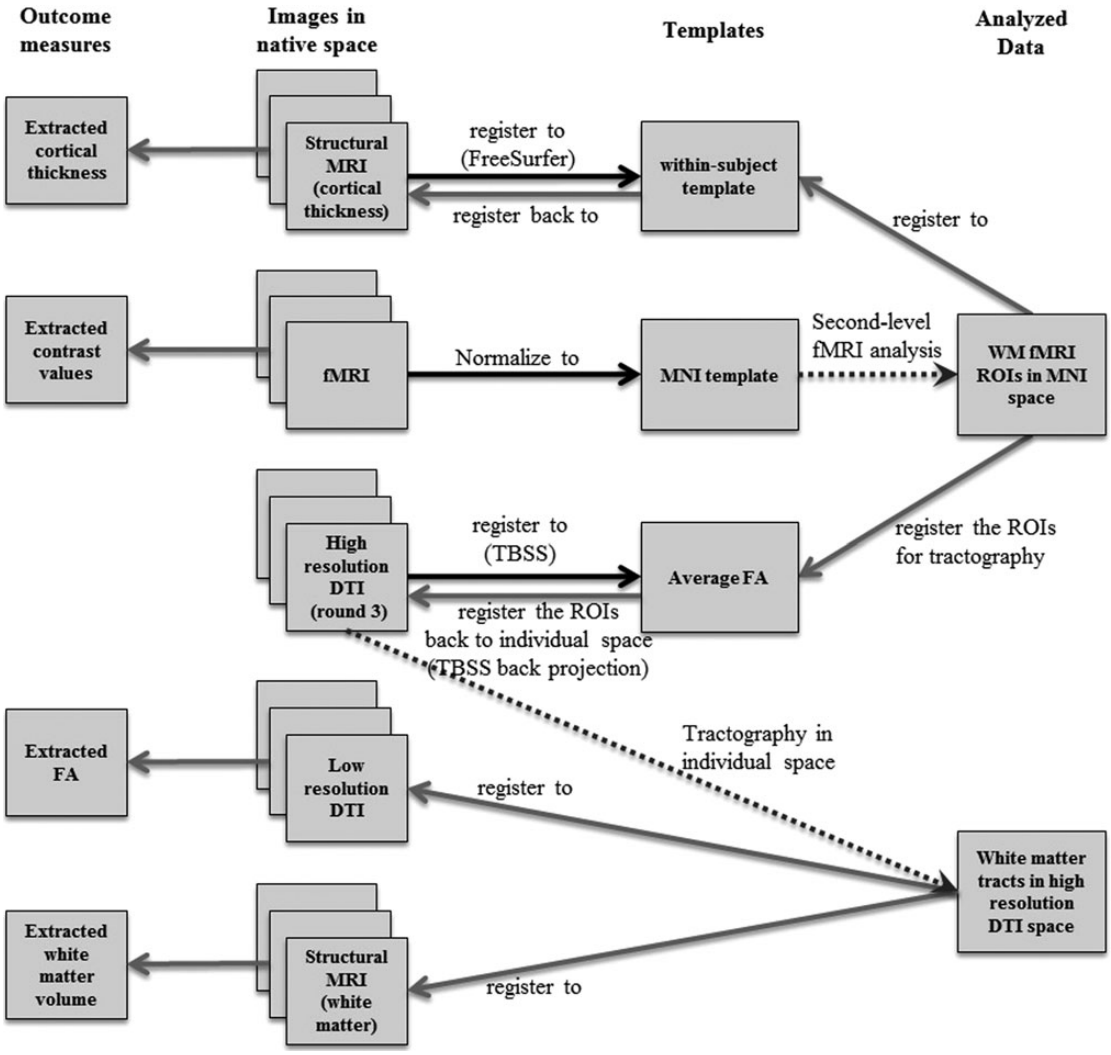

Figure 2. Image analysis and registration pipeline showing the registration between the native space and the template within each modality as well as the transformations between different modalities. Black and gray arrows show the registration and back projection transformations, respectively. The dotted arrows show the steps for fMRI second-level analysis as well as DTI tractography.

method for non-FA images and then binarized and averaged across all subjects. For visualization, the tractography results were finally thresholded at the group level by keeping the pathways that were present in 90% of the cases. The group-averaged maps of both the fronto-parietal and fronto-striatal networks are shown in Figure 2*B*, *C*.

To find the white matter pathways in each individual space, the white matter pathways traced by probabilistic tracking on high-resolution data were registered to the low-resolution longitudinal FA images. We then thresholded the tracts by 5% of the maximum number of samples and subsequently measured the mean FA values within this individual space, for all 3 rounds.

Structural Brain Imaging

T_1-weighted spin echo scans were collected using a 3-dimensional magnetization-prepared rapid gradient-echo sequence with TR = 2300 ms, TE = 2.92 ms, FOV of 256 × 256 mm^2, 256 × 256 matrix size, 176 sagittal slices, and 1 mm^3 isotropic voxel size. To speed up the acquisition, the GRAPPA parallel imaging (acceleration factor of 2) was also performed. The structural images were then processed with 2 different methods. The first technique was voxel-based morphometry (VBM), which segmented the brain into gray matter, white matter, and cerebral spinal fluid. The volume of white matter in the pathways of interest (the fronto-striatal and fronto-parietal) was computed using the white matter segmented images. The second technique was cortical thickness measurement using the freesurfer software (https://surfer.nmr.mgh.harvard.edu). This method was used for measuring the cortical thickness of the gray matter in the mentioned cortical ROIs.

Structural Brain Analysis: Voxel-Based Morphometry

VBM was performed on structural data collected across all 3 rounds of data collection using the SPM5, Diffeomorphic Anatomical Registration Through Exponentiated (DARTEL) toolbox. The modulated white matter segmented images were then smoothed with an 8-mm Gaussian kernel. The traced fronto-parietal and fronto-striatal tracts were first thresholded by 5% of their maximum value and then registered to the segmented white matter images, individually for all 3 time points. The averaged white matter volume in these 2 pathways was then computed to be used in the subsequent statistical analyses.

Structural Brain Analysis: Cortical Thickness Measurement

Cortical thickness of the structural dataset was estimated using automatic longitudinal stream in FreeSurfer (Reuter et al. 2012). This tool measures the thickness of the cortex by constructing models for the boundary between gray and white matter. First, a within-subject template was created for each subject using inverse consistent registration

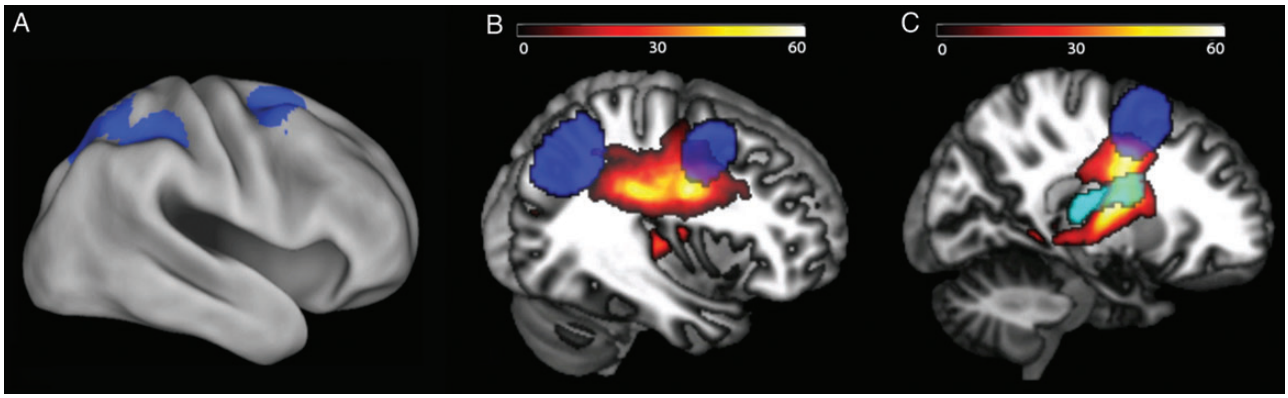

Figure 3. (*A*) Functionally active cortical regions (superior frontal, superior, and inferior parietal) during the performance on a visuo-spatial WM task. (*B*) Population map of the probabilistic fiber tracking of fronto-parietal pathways connecting superior frontal to intraparietal cortex. (*C*) Population map of fronto-striatal pathways, connecting caudate (shown by light blue) to the superior frontal ROI. The color bars correspond to the number of subjects with available white mater pathways.

(Reuter et al. 2010; Reuter and Fischl 2011). Then, several processing steps (Dale et al. 1999; Fischl and Dale 2000) including skull removing, template transformation, and atlas registration were performed. Images were later segmented to white matter, gray matter, and pial, based on intensity and neighborhood voxel restrictions. The distance between the white and the pial was computed as the thickness at each location of the cortex. The cortical thickness of the 2 particular cortical regions (superior frontal and intraparietal ROIs) was then calculated using the workflow described in http://surfer.nmr.mgh.harvard.edu/fswiki/VolumeRoiCorticalThickness.

ROI-Based Statistical Analyses

As the main aim of this research, the functional and structural ROI-based measures in the fronto-striatal and fronto-parietal networks were assessed for concurrent- and prediction-based correlations between brain–brain and brain–WM measures. The mean values of the WM functional contrast and cortical thickness were extracted from functionally active cortical regions during visuo-spatial WM task performance inside the scanner. Since the structural and functional measures in analogous areas were highly correlated (all $r > 0.84$), we averaged them in both the left and right hemispheres. The white matter volume and FA were also computed from the white matter pathways traced by probabilistic fiber tracking of fronto-parietal and fronto-striatal tracts. Visuo-spatial WM was the only behavioral measure in this study.

Cross-Sectional Analysis

To assess the concurrent correlations between brain and behavior measures, the ROI-based mean scores were analyzed using a mixed linear model in the IBM SPSS statistics 21.0 software with a restricted maximum likelihood (REML) method, considering 3 repeated measures and the "unstructured" type for repeated covariance. For brain–WM cross-sectional analysis, WM scores and brain measures were set as dependent variables and covariates of interest, respectively. Sex was also considered as a covariate. We did not control for the effect of age in the first set of analyses to keep the variations relating to the effects of age and related brain maturation. Later, in a separate analysis, we controlled for age to find the age-independent relationships.

Longitudinal Analysis

For the prediction analyses, the correlations between current to future measures were tested by the same model, mixed linear model; however the "compound symmetry" type was selected for the repeated covariance which assumes that the variance is constant across occasions (Fitzmaurice et al. 2012). In this case, we considered 2 repeated measures. For the first measures, the round 1 and 2 values were observed as current to future, respectively. And for the second measures, the round 2 and 3 were considered current to future values. Then, in a separate analysis, the model was corrected for the effect of sex as well as age at the current time point. The interaction with age was also assessed in the prediction analyses.

Results

The superior frontal and intraparietal cortical regions (Fig. 3*A*), as well as the caudate nucleus (shown with light blue in Fig. 3*C*), which were previously found active during performance on a visuo-spatial WM task (Dumontheil et al. 2011), were selected as seed ROI for fiber tracking of the fronto-parietal and fronto-striatal pathways. The averaged group map of the fronto-parietal tract is displayed sagittally in Figure 3*B* for the right hemisphere. The population map of the white matter pathways traced by probabilistic tractography of the voxels within caudate nucleus with the inclusion of superior frontal ROI is also shown in Figure 3*C*.

Cross-Sectional Analysis

The concurrent correlations between brain–WM and brain–brain measures were tested by the mixed linear model, including 3 repeated measures. The model was first tested without age correction. Then, in the further analysis, we corrected for the effect of age to see which of the concurrent relationships were age-independent.

Brain–WM Cross-Sectional Correlations

The estimated parameters, *F*, degrees of freedom (df), and *P*-values for the concurrent brain–WM relationships, are listed in Table 1 and are illustrated in Figure 4. BOLD contrast in both frontal and parietal areas correlated with current WM capacity ($P < 4.2 \times 10^{-4}$), whereas the correlation between the contrast values and the WM score was not significant for caudate nucleus. The volume of white matter and FA values in both fronto-parietal and fronto-striatal tracts correlated with the current WM score ($P < 1.7 \times 10^{-5}$ and $P < 7.4 \times 10^{-4}$, respectively). The cortical thickness of the functional ROIs in the parietal region negatively correlated with the current WM capacity ($P = 2.7 \times 10^{-3}$), whereas the thickness in superior frontal and the volume of the caudate nucleus did not correlate with the WM score. All the significant correlations survived the multiple comparisons correction for 10 tested correlations as listed in Table 1.

Out of the relationships that survived the multiple comparison corrections, FA values of the both fronto-parietal and fronto-striatal pathways ($P < 0.013$) as well as BOLD in cortical ROIs ($P < 0.027$) and the cortical thickness in superior frontal ($P = 0.020$) remained significant after the linear effect of age was removed. This shows that the correlations between these brain measures and WM capacity were not only related to brain maturation, but also to age-independent interindividual variations. We also tested removing the quadratic effect of age. The associations that survived this correction were the same as those marked by ** in Table 1.

Table 1
Correlation of brain measures with concurrent WM performance (cross-sectional analysis)

Imaging measures	Regions	Estimated parameters	*F* (df)	*P*-value
BOLD contrast values	Superior frontal*	3.55	13.02 (146.34)	**4.22×10^{-4}**
	Parietal**	3.25	30.16 (134.72)	**$<10^{-6}$**
	Caudate	2.55	2.91 (142.46)	0.09
Cortical thickness volume	Superior frontal*	5.36	2.65 (150.83)	0.11
	Parietal	−9.20	9.28 (108.89)	**2.66×10^{-3}**
White matter volume	Caudate	0.01	0.03 (113.85)	0.863
	Fronto-parietal	41.56	21.35 (68.99)	**1.70×10^{-5}**
	Fronto-striatal	46.51	24.14 (69.28)	**6.00×10^{-6}**
Fractional anisotropy	Fronto-parietal*	79.91	11.98 (120.93)	**7.41×10^{-4}**
	Fronto-striatal*	92.49	13.27 (119.68)	**4.00×10^{-4}**

P-values in bold indicate the significant relationships after correction for multiple comparisons of 10 tests ($P < 0.005$).
*, **Significant after the effect of age was removed.
*$P < 0.05$, not corrected for multiple comparisons.
**$P < 0.05$, corrected for multiple comparisons.

Brain–Brain Cross-Sectional Correlations

The estimated parameters, *F*, (df), and *P*-values, for the correlations between the concurrent brain–brain measures are listed in Table 2. Regarding the fronto-parietal network, cortical thickness of the parietal ROIs correlated with BOLD contrast values in the corresponding regions ($P = 4.6 \times 10^{-4}$, significant after multiple comparisons of 18 tests as listed in Table 2), though this relationship was not significant for the superior frontal ROI. In the assessment of the relationship between fMRI activity and white matter structure, the correlation between the volume of fronto-parietal pathways and contrast values in parietal area was significant, $P = 1.4 \times 10^{-3}$ (significant after multiple comparisons). Furthermore, the volume of caudate correlated significantly with both white matter volume and FA of the fronto-striatal pathway ($P = 0.039$ and 0.003, respectively).

In separate analyses, we corrected for the linear effect of age in order to assess which of the brain–brain relationships were due to age. The significant correlations between white matter volume and BOLD contrast as well as the cortical thickness remained significant for both networks, after removing the effect of age. We also tested removing the quadratic effect of age. The associations that survived this correction were the same as those marked by ** in Table 2. Relationships between FA and cortical measures were only significant for cortical thickness. BOLD to cortical thickness correlations were not significant after the effect of age was removed, which indicated an influence of age.

Longitudinal Analysis of Working Memory Capacity

Table 3 lists the estimated parameters of the correlations between current brain measures to future WM scores, including no covariates. We found that future WM capacity could be

Table 2
Concurrent correlations of brain–brain measures in fronto-parietal and fronto-striatal networks (cross-sectional analysis)

		BOLD contrast values					
		Superior frontal			Parietal		
		Estimated parameters	*F* (df)	*P*-value	Estimated parameters	*F* (df)	*P*-value
Cortical thickness	Superior frontal	−0.26	1.32 (143.16)	0.25	—	—	—
	Parietal	—	—	—	−0.98	12.99 (113.03)	**4.65×10^{-4}**
		White matter volume					
		Fronto-parietal			Fronto-striatal		
		Estimated parameters	*F* (df)	*P*-value	Estimated parameters	*F* (df)	*P*-value
BOLD contrast values	Superior frontal*	0.01	3.12 (33.68)	0.09	0.02	3.47 (34.24)	0.07
	Parietal*	0.01	11.88 (35.52)	**1.47×10^{-3}**	—	—	—
	Caudate*	—	—	—	0.01	3.22 (38.51)	0.08
Cortical thickness volume	Superior frontal*	0.04	5.99 (43.02)	**0.02**	0.04	6.16 (42.86)	**0.02**
	Parietal*	−0.01	0.18 (43.46)	0.65	—	—	—
	Caudate**	—	—	—	0.01	4.37 (91.87)	**0.04**
		Fractional anisotropy					
		Fronto-parietal			Fronto-striatal		
		Estimated parameters	*F* (df)	*P*-value	Estimated parameters	*F* (df)	*P*-value
BOLD contrast values	Superior frontal	0.01	2.78 (93.62)	0.09	0.02	4.38 (65.48)	0.04
	Parietal	0.02	0.54 (84.55)	0.46	—	—	—
	Caudate*	—	—	—	0.01	4.55 (58.20)	**0.04**
Cortical thickness volume	Superior frontal*	0.03	7.51 (98.25)	**7.31×10^{-3}**	0.02	3.66 (148.53)	0.06
	Parietal	0.02	2.14 (100.07)	0.146	—	—	—
	Caudate*	—	—	—	0.01	9.23 (62.23)	**3.48×10^{-3}**

P-values in bold indicate the significant relationships after correction for multiple comparisons of 18 tests ($P < 0.0027$).
*, **Significant after the effect of age was removed.
*$P < 0.05$, not corrected for multiple comparisons.
**$P < 0.05$, corrected for multiple comparisons.

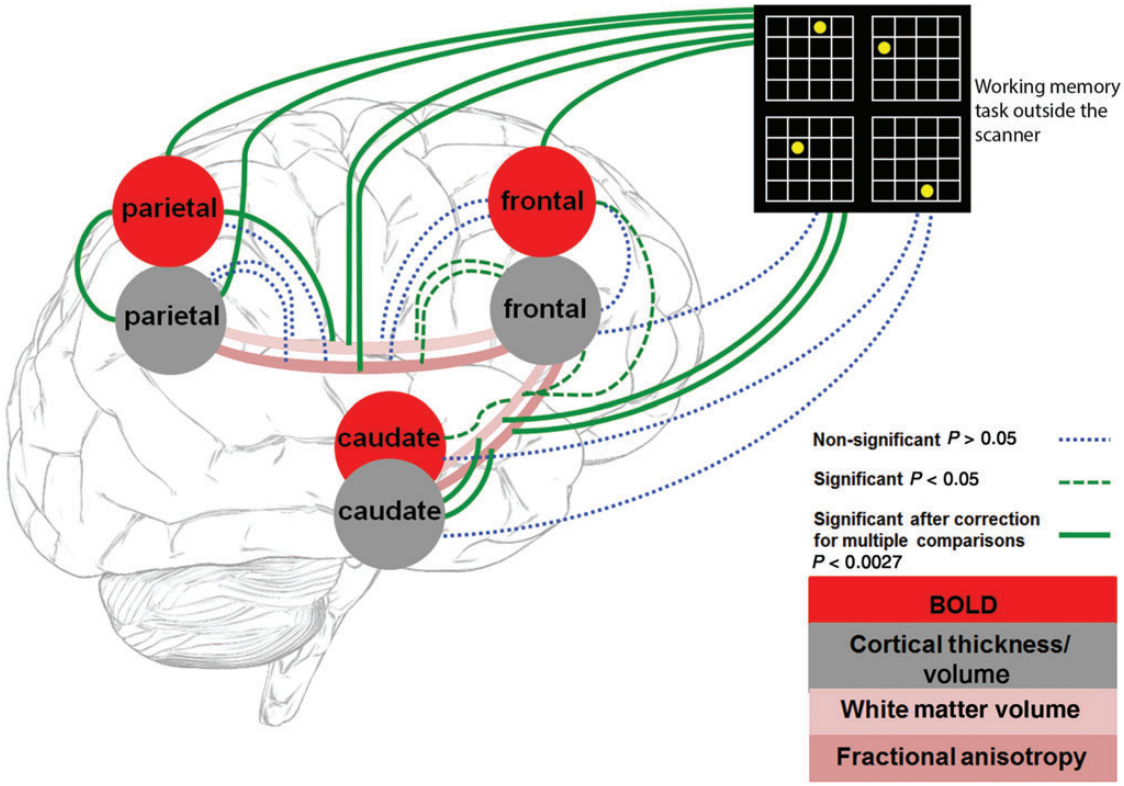

Figure 4. Cross-sectional analysis of correlations between brain–brain and brain–WM. The correlations include all 3 rounds of repeated measures for all variables. The dashed green and dotted blue lines show the significant and nonsignificant correlations, respectively, based on Tables 1 and 2. The thick green lines are those that survived the multiple comparisons correction.

Table 3
Prediction of future WM capacity based on measures collected 2 years earlier

Imaging measures	Regions	Estimated parameters	*F* (df)	*P*-value
BOLD contrast values	Superior frontal	2.33	2.68 (73.89)	0.11
	Parietal	1.67	2.98 (78.43)	0.09
	Caudate	6.30	7.58(73.43)	**7.4×10^{-3}**
Cortical thickness	Superior frontal	6.23	2.67 (93.51)	0.11
	Parietal	−2.72	0.39 (104.93)	0.53
	Caudate	0.01	1.84 (81.13)	0.18
White matter volume	Fronto-parietal	27.26	7.24 (48.07)	**0.010**
	Fronto-striatal	30.69	8.44 (47.73)	**5.55×10^{-3}**
Fractional anisotropy	Fronto-parietal **	105.57	17.96 (71.33)	**6.60×10^{-5}**
	Fronto-striatal**	156.96	26.96 (72.52)	**2.00×10^{-6}**

The *P*-values in bold correspond to the tests that survived correction for multiple comparisons.
**Significant after the effect of age was removed ($P < 0.05$, corrected for multiple comparisons).

predicted by white matter structural measures in both fronto-parietal and fronto-striatal pathways (for white matter volume: $P < 0.01$ and for FA: $P < 6.6 \times 10^{-5}$). Moreover, BOLD contrast in the caudate significantly predicted future WM performance ($P = 7.4 \times 10^{-3}$).

In a separate analysis, we corrected for sex and age at baseline. The FA values of both fronto-parietal and fronto-striatal pathways still significantly predicted future WM performance, $P < 6.8 \times 10^{-3}$ (significant after correction for multiple comparisons). However, white matter volume and caudate BOLD activity were not significant after controlling for age. This is consistent with the concurrent correlations after correcting for age, in which we found that only white matter FA values were age-independently correlated with WM.

We also analyzed the interaction with age in the prediction analyses. The only brain measure that showed significant interaction with age was the activity in caudate nucleus ($P = 1.8 \times 10^{-4}$). Then, we divided the subjects into 2 groups based on their age (below and above 16 years old) to test the predictive ability of caudate activity in these 2 subsets. The BOLD contrast values in caudate significantly predicted future WM capacity for younger subjects ($P = 9.0 \times 10^{-4}$) but not for older individuals ($P = 0.24$), after controlling for age and sex.

Discussion

In the present study, we investigated the relationship between brain structure and function in an anatomically predefined network related to WM performance, using both cross-sectional and longitudinal designs.

In the cross-sectional analysis, WM capacity correlated with BOLD contrast in both frontal and parietal regions, cortical thickness in the parietal cortex, and white matter structure (both FA and volume) of fronto-parietal and fronto-striatal tracts. These findings are consistent with previous developmental studies of BOLD activity (Klingberg et al. 2002; Kwon et al. 2002; Olesen, Nagy, et al. 2003; Crone et al. 2006; Klingberg 2006; Scherf et al. 2006). Cortical thinning of the supramarginal gyrus has previously been correlated with performance on a verbal WM task in a developmental sample, after correction for age (Østby et al. 2011).

Correlation between white matter structure and WM capacity is consistent with several previous developmental studies (Olesen, Nagy, et al. 2003; Nagy et al. 2004; Østby et al. 2011; Vestergaard et al. 2011). FA of the ventrofronto-striatal tract has previously been correlated with the development of response inhibition (Liston et al. 2006), but to our knowledge the fronto-striatal tract has not been associated with WM capacity.

ADHD is a neuropsychiatric disorder where WM deficits are thought to play an important role (Nigg 2001; Westerberg et al. 2004; Martinussen et al. 2005). The current associations with WM are largely overlapping with findings in ADHD subjects of thinner frontal and parietal cortex (Makris et al. 2007) as well as lower FA and fronto-parietal connections (Makris et al. 2008), suggesting that these anatomical deviations observed in ADHD could be related to cognitive impairments.

In this study, we provided results both with and without accounting for the effect of age, because correcting for age has both advantages and disadvantages. The key reason to correct for age would be to remove possible nonspecific effects of development. In the case of WM, that would be assuming that there is some factor outside the measured WM network of brain regions that is responsible for the increase in WM capacity, and that this unknown factor correlates with age. The disadvantage of correcting for age is that it only leaves variance that is independent of development, which defeats the purpose of using a developmental sample in the first place. We would thus argue that not co-varying out the effect of age gives a better estimate of the developmental aspect of WM development. The age-independent correlation, in this case the FA values of the fronto-parietal and fronto-striatal networks as well BOLD in parietal cortex, would be factors contributing to interindividual differences in WM capacity independent of development. This is also consistent with reports of such association in adult samples (Takeuchi et al. 2011).

Regarding the white matter measures and their relationship to current and future WM capacity, there was a difference in that FA values, but not volume, were significant after correcting for age. The white matter measures could be affected by many structural characteristics, such as the number, size, diameter, packing and organization of the axons, oligodendrocytes, and other extra-neuronal factors such as astrocyte changes and angiogenesis. In this study, we found that FA is less affected than white matter volume by age. If FA is less affected by age, one might speculate that the remaining relationship is influenced by some structural aspects, which do not increase with age and might be due to the genetic differences such as the number, packing, and organization of axons.

The cross-sectional analysis showed regional correlations of BOLD, cortical thickness, and FA. Correlations between fronto-parietal BOLD and FA values have previously been reported in developmental samples (Olesen, Nagy, et al. 2003; Østby et al. 2011) as well as adult samples (Burzynska et al. 2011). In another study, the relationship between the structural connection probabilities and its functional activation was trained in a least-squares linear regression model and could predict functional activation to faces in the fusiform gyrus (Saygin et al. 2011). It is also possible that the BOLD-cortical thickness correlations, as also found in adults studies (Takeuchi et al. 2014), reflect a causal influence of cortex thickness on brain activity. Regarding the relationship to white matter structures, it is difficult to directly interpret these as a causal relationship, since we did not include additional control regions outside of the WM network, and could not find evidence of any structural characteristics predicting other structural measures 2 years later (data not shown).

The longitudinal analysis provided a radically different pattern of associations. Despite being correlated with concurrent WM capacity, none of the cortical measures, neither BOLD nor thickness, predicted future WM. White matter structure, on the other hand, correlated with both concurrent measures of WM and WM capacity 2 years later. These results clearly show how the white matter integrity, specifically of fronto-parietal and fronto-striatal tracts, provides an important basis for the development of future WM capacity. The present data might suggest that the development of capacity would only emerge in connection with other regions, and the efficiency of those connections determine the rate of development.

The measures from the caudate nucleus provided a very different pattern of association with WM than all other structures: while neither volume nor activity correlated with concurrent WM, there was a significant correlation between caudal activity and WM capacity 2 years later. The importance of the caudate is also illustrated by the predictive function of the fronto-striatal connections. Moreover, there was a significant interaction of caudal activity by age, emphasizing its role in early development.

Although the caudate nucleus is connected to the prefrontal and parietal cortices (Alexander et al. 1991; Aosaki et al. 1995) and active during performance on a WM task in both nonhuman primates (Levy et al. 1997), children (Klingberg et al. 2002; Ziermans et al. 2012), and adults (McNab and Klingberg 2007), it has not specifically been related to childhood development of WM. Regarding memory and cognitive function, the caudate has mostly been linked to implicit learning and habit formation (Packard and Knowlton 2002; Graybiel 2008). In a study where nonhuman primates learned associations in a delay task, it was found that, after the rule changed, the activation of the caudate changed earlier than the cortical changes, where the latter matched the changes in behavior (Pasupathy and Miller 2005). This is consistent with the current finding where cortical activity and structure correlate with behavior, but are preceded in time by the activity of the caudate.

Studies of the neural basis of WM training (Klingberg et al. 2005; Klingberg 2010) might provide a link between the studies of implicit learning on the one hand, and cognitive development on the other. Two studies of training-induced improvements in WM have shown activity in the thalamus and caudate nucleus (Olesen, Westerberg, et al. 2003; Dahlin et al. 2008), and in one of those, the striatal activity predicted the amount of improvement seen after training (Dahlin et al. 2008). In a positron emission tomography study, improvements after WM training were associated with changes in D2 receptor occupancy of the caudate (Bäckman et al. 2011), while the change in capacity is associated with cortical D1 receptor density (McNab and Klingberg 2007). Genetic studies have found that polymorphisms related to the *DAT-1* transporter (Brehmer et al. 2009; Söderqvist et al. 2012) and *DRD2* receptor expression (Söderqvist et al. 2014) affect the amount of improvement during WM training. Both *DAT-1* and *DRD2* are preferentially expressed in the basal ganglia. Taken together, these findings suggest that there might be similarities between cognitive development during childhood, training of WM, and implicit learning, and that the caudate nucleus and the fronto-striatal

connections play a key role in the learning processes, while the capacity is more closely related to cortical processes.

In conclusion, these results suggest a dynamic of the neural systems underlying WM development, where cortical activity and structure are closely related to current WM, while the subcortical white matter tracts and activity in the caudate are preceding these changes and predict future WM capacity.

Notes

Conflict of Interest: None declared.

References

Alexander GE, Crutcher MD, DeLong MR. 1991. Basal ganglia-thalamocortical circuits: parallel substrates for motor, oculomotor, "prefrontal" and "limbic" functions. Prog Brain Res. 85:119–146.

Alloway T. 2007. Automated working memory assessment manual. Oxford: Harcourt.

Aosaki T, Kimura M, Graybiel A. 1995. Temporal and spatial characteristics of tonically active neurons of the primate's striatum. J Neurophysiol. 73:1234–1252.

Bäckman L, Nyberg L, Soveri A, Johansson J, Andersson M, Dahlin E, Neely AS, Virta J, Laine M, Rinne JO. 2011. Effects of working-memory training on striatal dopamine release. Science. 333:718.

Brehmer Y, Westerberg H, Bellander M, Fürth D, Karlsson S, Bäckman L. 2009. Working memory plasticity modulated by dopamine transporter genotype. Neurosci Lett. 467:117–120.

Brett M, Anton J-L, Valabregue R, Poline J-B. 2002. Region of interest analysis using the MarsBar toolbox for SPM 99. Neuroimage. 16: S497.

Burzynska AZ, Nagel IE, Preuschhof C, Li S-C, Lindenberger U, Bäckman L, Heekeren HR. 2011. Microstructure of frontoparietal connections predicts cortical responsivity and working memory performance. Cereb Cortex. 21:2261–2271.

Camos V. 2008. Low working memory capacity impedes both efficiency and learning of number transcoding in children. J Exp Child Psychol. 99:37–57.

Crone EA, Wendelken C, Donohue S, van Leijenhorst L, Bunge SA. 2006. Neurocognitive development of the ability to manipulate information in working memory. Proc Natl Acad Sci. 103:9315–9320.

Dahlin E, Neely AS, Larsson A, Bäckman L, Nyberg L. 2008. Transfer of learning after updating training mediated by the striatum. Science. 320:1510–1512.

Dale AM, Fischl B, Sereno MI. 1999. Cortical surface-based analysis: I. Segmentation and surface reconstruction. Neuroimage. 9:179–194.

Dumontheil I, Klingberg T. 2012. Brain activity during a visuospatial working memory task predicts arithmetical performance 2 years later. Cereb Cortex. 22:1078–1085.

Dumontheil I, Roggeman C, Ziermans T, Peyrard-Janvid M, Matsson H, Kere J, Klingberg T. 2011. Influence of the COMT genotype on working memory and brain activity changes during development. Biol Psychiatry. 70:222–229.

Fischl B, Dale AM. 2000. Measuring the thickness of the human cerebral cortex from magnetic resonance images. Proc Natl Acad Sci. 97:11050–11055.

Fitzmaurice GM, Laird NM, Ware JH. 2012. Applied longitudinal analysis. John Wiley and Sons.

Gathercole SE, Brown L, Pickering SJ. 2003. Working memory assessments at school entry as longitudinal predictors of National Curriculum attainment levels. Educ Child Psychol. 20:109–122.

Graybiel AM. 2008. Habits, rituals, and the evaluative brain. Annu Rev Neurosci. 31:359–387.

Klingberg T. 2006. Development of a superior frontal? Intraparietal network for visuo-spatial working memory. Neuropsychologia. 44:2171–2177.

Klingberg T. 2010. Training and plasticity of working memory. Trends Cogn Sci. 14:317–324.

Klingberg T, Fernell E, Olesen PJ, Johnson M, Gustafsson P, Dahlström K, Gillberg CG, Forssberg H, Westerberg H. 2005. Computerized training of working memory in children with ADHD—a randomized, controlled trial. J Am Acad Child Adolesc Psychiatry. 44:177–186.

Klingberg T, Forssberg H, Westerberg H. 2002. Increased brain activity in frontal and parietal cortex underlies the development of visuospatial working memory capacity during childhood. J Cogn Neurosci. 14:1–10.

Kwon H, Reiss AL, Menon V. 2002. Neural basis of protracted developmental changes in visuo-spatial working memory. Proc Natl Acad Sci. 99:13336–13341.

Leh SE, Johansen-Berg H, Ptito A. 2006. Unconscious vision: new insights into the neuronal correlate of blindsight using diffusion tractography. Brain. 129:1822–1832.

Levy R, Friedman HR, Davachi L, Goldman-Rakic PS. 1997. Differential activation of the caudate nucleus in primates performing spatial and nonspatial working memory tasks. J Neurosci. 17:3870–3882.

Liston C, Watts R, Tottenham N, Davidson MC, Niogi S, Ulug AM, Casey B. 2006. Frontostriatal microstructure modulates efficient recruitment of cognitive control. Cereb Cortex. 16:553–560.

Makris N, Biederman J, Valera EM, Bush G, Kaiser J, Kennedy DN, Caviness VS, Faraone SV, Seidman LJ. 2007. Cortical thinning of the attention and executive function networks in adults with attention-deficit/hyperactivity disorder. Cereb Cortex. 17:1364–1375.

Makris N, Buka SL, Biederman J, Papadimitriou GM, Hodge SM, Valera EM, Brown AB, Bush G, Monuteaux MC, Caviness VS. 2008. Attention and executive systems abnormalities in adults with childhood ADHD: a DT-MRI study of connections. Cereb Cortex. 18:1210–1220.

Martinussen R, Hayden J, Hogg-Johnson S, Tannock R. 2005. A meta-analysis of working memory impairments in children with attention-deficit/hyperactivity disorder. J Am Acad Child Adolesc Psychiatry. 44:377–384.

McLean JF, Hitch GJ. 1999. Working memory impairments in children with specific arithmetic learning difficulties. J Exp Child Psychol. 74:240–260.

McNab F, Klingberg T. 2007. Prefrontal cortex and basal ganglia control access to working memory. Nat Neurosci. 11:103–107.

Nagy Z, Westerberg H, Klingberg T. 2004. Maturation of white matter is associated with the development of cognitive functions during childhood. J Cogn Neurosci. 16:1227–1233.

Nigg JT. 2001. Is ADHD a disinhibitory disorder? Psychol Bull. 127:571.

Olesen PJ, Macoveanu J, Tegnér J, Klingberg T. 2007. Brain activity related to working memory and distraction in children and adults. Cereb Cortex. 17:1047–1054.

Olesen PJ, Nagy Z, Westerberg H, Klingberg T. 2003. Combined analysis of DTI and fMRI data reveals a joint maturation of white and grey matter in a fronto-parietal network. Cogn Brain Res. 18: 48–57.

Olesen PJ, Westerberg H, Klingberg T. 2003. Increased prefrontal and parietal activity after training of working memory. Nat Neurosci. 7:75–79.

Østby Y, Tamnes CK, Fjell AM, Walhovd KB. 2011. Morphometry and connectivity of the fronto-parietal verbal working memory network in development. Neuropsychologia. 49:3854–3862.

Packard MG, Knowlton BJ. 2002. Learning and memory functions of the basal ganglia. Annu Rev Neurosci. 25:563–593.

Pasupathy A, Miller EK. 2005. Different time courses of learning-related activity in the prefrontal cortex and striatum. Nature. 433:873–876.

Postle BR, Zarahn E, D'Esposito M. 2000. Using event-related fMRI to assess delay-period activity during performance of spatial and nonspatial working memory tasks. Brain Res Protoc. 5:57–66.

Reuter M, Fischl B. 2011. Avoiding asymmetry-induced bias in longitudinal image processing. Neuroimage. 57:19–21.

Reuter M, Rosas HD, Fischl B. 2010. Highly accurate inverse consistent registration: a robust approach. Neuroimage. 53:1181–1196.

Reuter M, Schmansky NJ, Rosas HD, Fischl B. 2012. Within-subject template estimation for unbiased longitudinal image analysis. Neuroimage. 61:1402–1418.

Saygin ZM, Osher DE, Koldewyn K, Reynolds G, Gabrieli JD, Saxe RR. 2011. Anatomical connectivity patterns predict face selectivity in the fusiform gyrus. Nat Neurosci. 15:321–327.
Scherf KS, Sweeney JA, Luna B. 2006. Brain basis of developmental change in visuospatial working memory. J Cogn Neurosci. 18:1045–1058.
Shaw P, Greenstein D, Lerch J, Clasen L, Lenroot R, Gogtay N, Evans A, Rapoport J, Giedd J. 2006. Intellectual ability and cortical development in children and adolescents. Nature. 440:676–679.
Söderqvist S, Bergman Nutley S, Peyrard-Janvid M, Matsson H, Humphreys K, Kere J, Klingberg T. 2012. Dopamine, working memory, and training induced plasticity: Implications for developmental research. Dev Psychol. 48:836.
Söderqvist S, Matsson H, Peyrard-Janvid M, Kere J, Klingberg T. 2004. Polymorphisms in the dopamine receptor 2 gene region influence improvements during working memory training in children and adolescents. J Cogn Neurosci. 26:56–62.
Söderqvist S, McNab F, Peyrard-Janvid M, Matsson H, Humphreys K, Kere J, Klingberg T. 2010. The SNAP25 gene is linked to working memory capacity and maturation of the posterior cingulate cortex during childhood. Biol Psychiatry. 68:1120–1125.
Sowell ER, Thompson PM, Leonard CM, Welcome SE, Kan E, Toga AW. 2004. Longitudinal mapping of cortical thickness and brain growth in normal children. J Neurosci. 24:8223–8231.
Szucs D, Devine A, Soltesz F, Nobes A, Gabriel F. 2013. Developmental dyscalculia is related to visuo-spatial memory and inhibition impairment. Cortex. 49:2674–2688.
Takeuchi H, Taki Y, Nouchi R, Hashizume H, Sassa Y, Sekuguchi A, Kotozaki Y, Nakagawa S, Nagase T, Miyauchi CM. 2014. Associations among imaging measures (2): The association between gray matter concentration and task-induced activation changes. Hum Brain Mapp. 35:185–198.
Takeuchi H, Taki Y, Sassa Y, Hashizume H, Sekiguchi A, Fukushima A, Kawashima R. 2011. Verbal working memory performance correlates with regional white matter structures in the frontoparietal regions. Neuropsychologia. 49:3466–3473.
Tamnes CK, Fjell AM, Østby Y, Westlye LT, Due-Tønnessen P, Bjørnerud A, Walhovd KB. 2011. The brain dynamics of intellectual development: Waxing and waning white and gray matter. Neuropsychologia. 49:3605–3611.
Tamnes CK, Østby Y, Walhovd KB, Westlye LT, Due-Tønnessen P, Fjell AM. 2010. Neuroanatomical correlates of executive functions in children and adolescents: a magnetic resonance imaging (MRI) study of cortical thickness. Neuropsychologia. 48:2496–2508.
Tamnes CK, Walhovd KB, Grydeland H, Holland D, Ostby Y, Dale AM, Fjell AM. 2013. Longitudinal working memory development is related to structural maturation of frontal and parietal cortices. J Cogn Neurosci. 25:1611–1623.
Ullman H, Almeida R, Klingberg T. 2014. Structural maturation and brain activity predict future working memory capacity during childhood development. J Neurosci.
Vestergaard M, Madsen KS, Baaré WF, Skimminge A, Ejersbo LR, Ramsøy TZ, Gerlach C, Åkeson P, Paulson OB, Jernigan TL. 2011. White matter microstructure in superior longitudinal fasciculus associated with spatial working memory performance in children. J Cogn Neurosci. 23:2135–2146.
Wendelken C, O'Hare ED, Whitaker KJ, Ferrer E, Bunge SA. 2011. Increased functional selectivity over development in rostrolateral prefrontal cortex. J Neurosci. 31:17260–17268.
Westerberg H, Hirvikoski T, Forssberg H, Klingberg T. 2004. Visuo-spatial working memory span: a sensitive measure of cognitive deficits in children with ADHD. Child Neuropsychol. 10: 155–161.
Ziermans T, Dumontheil I, Roggeman C, Peyrard-Janvid M, Matsson H, Kere J, Klingberg T. 2012. Working memory brain activity and capacity link MAOA polymorphism to aggressive behavior during development. Transl Psychiatry. 2:e85.